

Plant Communications, Volume 3

Supplemental information

***OPAQUE3*, encoding a transmembrane bZIP transcription factor, regulates endosperm storage protein and starch biosynthesis in rice**

Ruijie Cao, Shaolu Zhao, Guiai Jiao, Yingqing Duan, Liuyang Ma, Nannan Dong, Feifei Lu, Mingdong Zhu, Gaoneng Shao, Shikai Hu, Zhonghua Sheng, Jian Zhang, Shaoqing Tang, Xiangjin Wei, and Peisong Hu

Supplemental Information:

OPAQUE3, encoding a transmembrane bZIP transcription factor, regulates endosperm storage protein and starch biosynthesis in rice

Ruijie Cao^{1,3}, Shaolu Zhao^{1,2,3}, Guiai Jiao¹, Yingqing Duan¹, Liuyang Ma¹, Nannan Dong¹, Feifei Lu¹, Mingdong Zhu¹, Gaoneng Shao¹, Shikai Hu¹, Zhonghua Sheng¹, Jian Zhang¹, Shaoqing Tang¹, Xiangjin Wei^{1,*}, Peisong Hu^{1,*}

¹ State Key Laboratory of Rice Biology, China National Center for Rice Improvement, China National Rice Research Institute, Hangzhou, 310006, China

² Institute of Agricultural Science in Jiangsu Coastal Areas, Yancheng, 224002, China

³ These authors contributed equally to this work.

* Correspondence: Xiangjin Wei (weixiangjin@caas.cn), Peisong Hu (peisonghu@126.com, hupeisong@caas.cn)

Supplemental Figures 1-14

Supplemental Tables 1

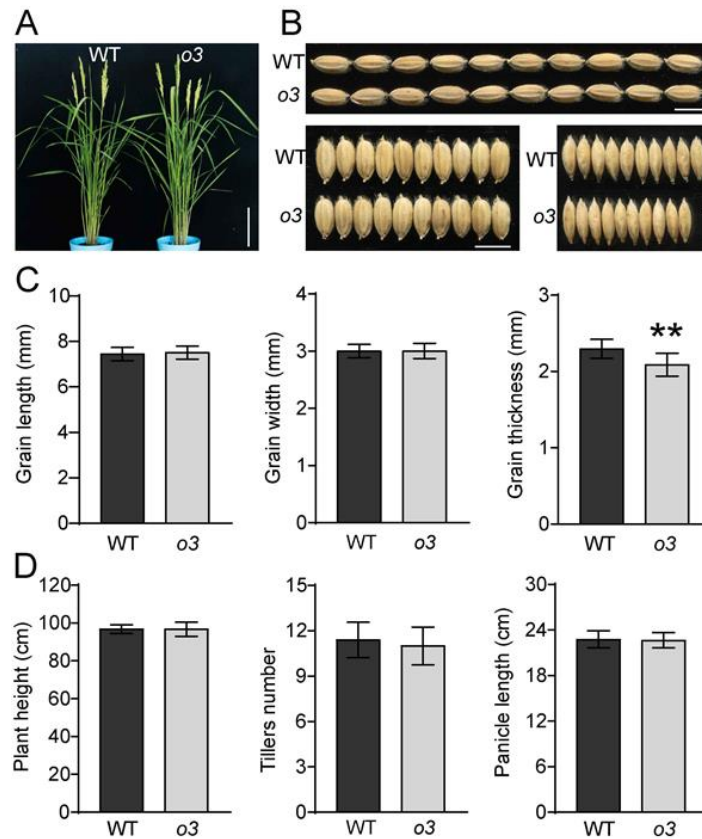


Figure S1. Characteristics of wild type (WT) and *o3* mutant.

(A) The plant phenotype of WT and *o3* after heading.

(B, C) The morphology **(B)** and Statistics **(C)** of grain length, grain width and grain thickness of WT and *o3* (n=200). Scale bars, 20 cm in **(A)**; 6mm in **(B)**.

(D) Plant height, tiller number and panicle length of WT and *o3*. Values are means \pm SD from three biological replicates, not less than 10 plants in each replication. The asterisks indicate statistical significance compared with the wild type, as determined by Student's *t*-test (**, $P < 0.01$).

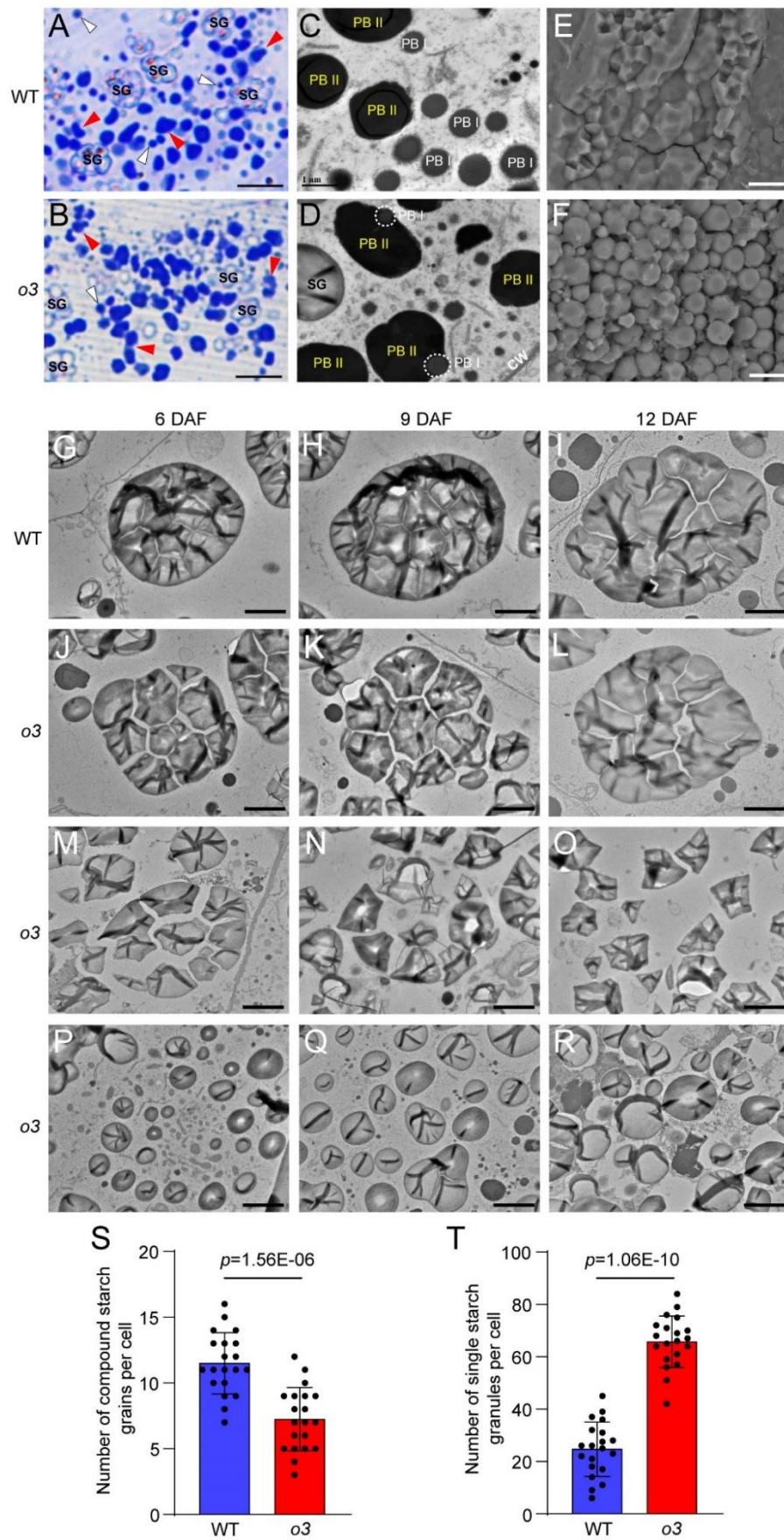


Figure S2. The morphology of protein body and starch granule in developing endosperm cells of wild type and *o3*.

(A, B) Semi-thin sections stained with Coomassie blue showing the morphology of PB I and PB II of WT and *o3* endosperm at 12 DAF. White arrowhead denotes PB I, red arrowhead denotes PB II; SG, starch granule. Scale bars, 20 μ m.

(C, D) Transmission electron microscopy showing the structure of PBI and PBII of WT and *o3* endosperm, White dotted line indicates the abnormal infusion of PBI and PBII. CW, cell wall. Scale bars, 1 μ m.

(E, F) Scanning electron microscopy images of transverse sections of mature grains of WT and *o3*. Scale bars, 10 μ m.

(G-I) Transmission electron microscopy (TEM) showed the well-developed amyloplast in WT endosperm cells at 6 DAF (**G**), 9 DAF (**H**), and 12 DAF (**I**). Scale bars, 2 μ m.

(J-L) Few well-developed amyloplast were observed in *o3* endosperm cells at 6 DAF (**J**), 9 DAF (**K**) and 12 DAF (**L**). Scale bars, 2 μ m.

(M-O) The amyloplasts were gradually disintegrated in *o3* endosperm cells from 6 DAF (**M**) to 9 DAF (**N**) and 12 DAF (**O**). Scale bars, 2 μ m.

(P-R) Single and dispersive starch granules in *o3* endosperm cells at 6 DAF (**P**), 9 DAF (**Q**), and 12 DAF (**R**). Scale bars, 2 μ m.

(S, T) Statistics of the number of starch compound grains and single granules in central endosperm cells of WT and *o3* at 9 DAF. Data are means \pm SD from at least three biological replicates. Statistically significant differences were determined using Student's *t*-test. *P*-values are shown when statistically significant.

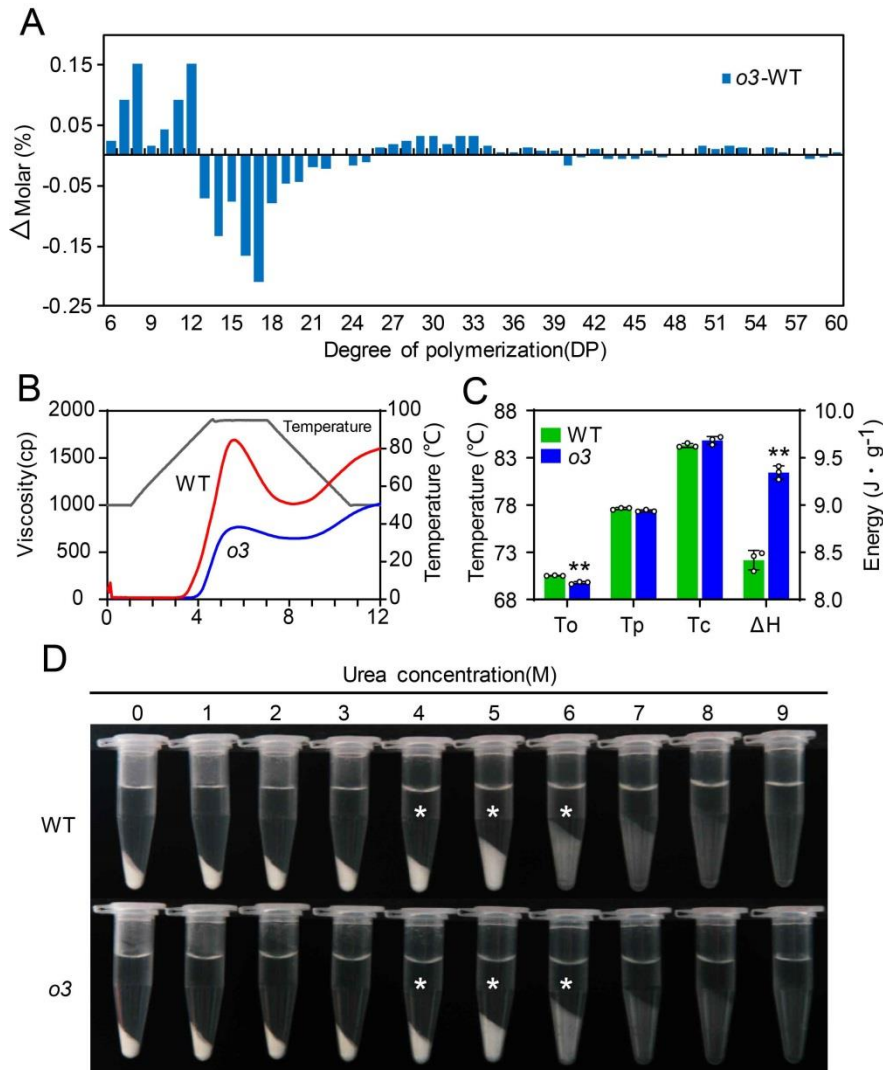


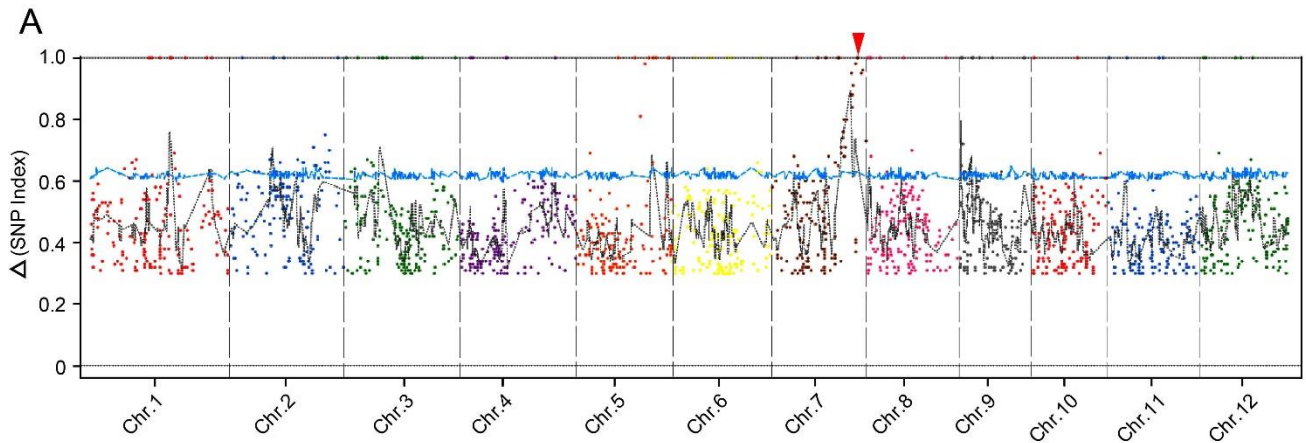
Figure S3. Starch physicochemical characteristics in the *o3* mutant.

(A) Differences in the amylopectin chain length distributions between the WT and *o3*.

(B) Pasting properties analyzing with a rapid visco analyzer (RVA) of endosperm starch of WT (red line) and *o3* (blue line). The viscosity value at each temperature is the average of three replicates. The gray line indicates the temperature changes during the measurements.

(C) Gelatinization temperature of endosperm starch. To, Tp, and Tc represent the onset, peak, and conclusion gelatinization temperatures, respectively. All data are presented as means \pm SD from three replicates. Statistically significant differences were determined using Student's *t*-test (**, $P < 0.01$).

(D) Gelatinization characteristics of starch from *o3* mutant seeds. Starch powder was mixed with different concentrations (1~9 M) of urea solution. The most significant difference was observed for 4~6 M urea (indicated by *).



B

SNP	Position	Genotype	Δ (SNP-index)	Variant	Gene	Description
SNP1	26610760	C to T	1	synonymous SNV	LOC_Os07g44560	AMP-binding domain containing protein
SNP2	26810333	T to C	1	nonsynonymous SNV	LOC_Os07g44950	bZIP transcription factor
SNP3	26108114	C to T	0.98	intronic	LOC_Os07g43610	hypothetical protein
SNP4	28371212	C to T	0.96	upstream	LOC_Os07g47460	expressed protein
SNP5	24796636	C to T	0.95	intronic	LOC_Os07g41380	retrotransposon protein
SNP6	27900815	C to T	0.95	intronic	LOC_Os07g46680	expressed protein
SNP7	25293558	C to T	0.91	splicing	LOC_Os07g42260	OsPAA2
SNP8	24593986	T to C	0.88	intronic	LOC_Os07g41090	HDA713
SNP9	25101693	C to T	0.88	intronic	LOC_Os07g41900	expressed protein
SNP10	24969228	T to A	0.84	upstream	LOC_Os07g41660	expressed protein
SNP11	20252223	T to C	0.81	intergenic	LOC_Os05g34210	expressed protein
SNP12	23272328	G to A	0.8	upstream	LOC_Os07g38780	transposon protein
SNP13	22518789	C to T	0.8	dow nstream	LOC_Os07g37580	diacylglycerol kinase

Figure S4. Mut-map cloning of *O3*.

(A) Distribution of progeny Δ (SNP-index) on chromosomes of the whole genome generated using Mut-map method. The black curves represent SNP-index plot regression lines; red arrowhead indicates the SNP located on candidate gene.

(B) The annotation of 13 candidate SNPs on chromosome 7 with SNP-index more than 0.8. The candidate SNP was shown in red format.

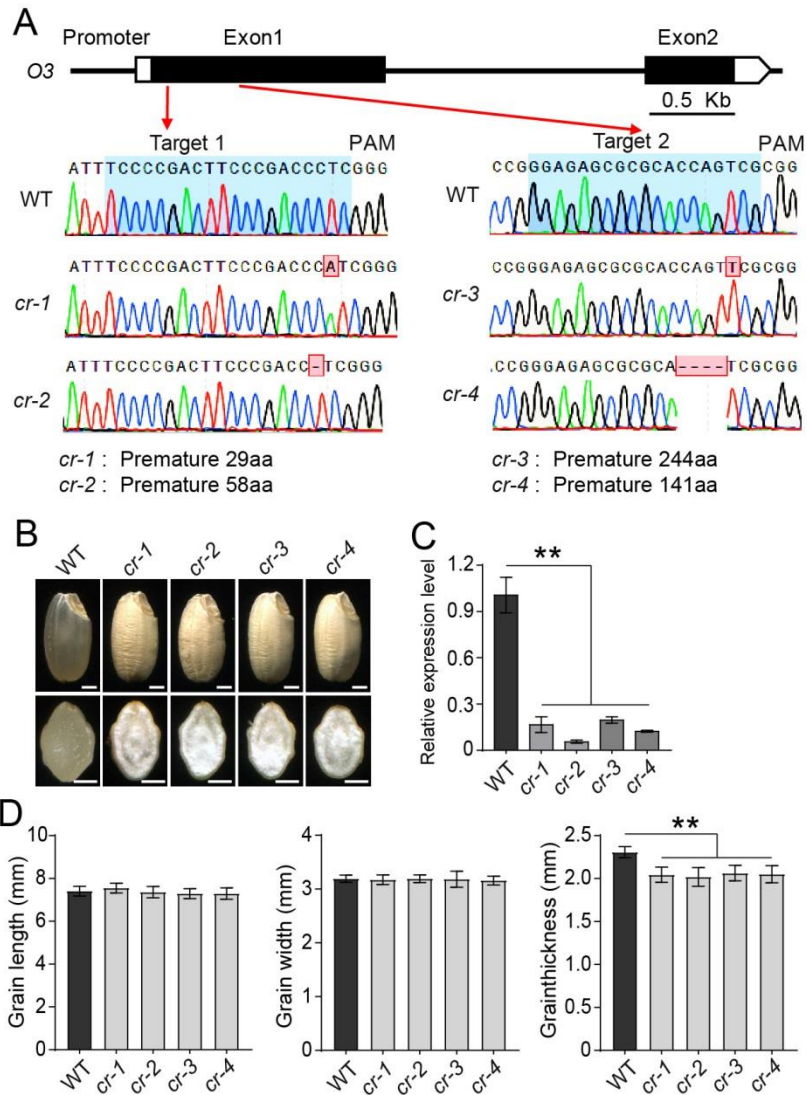


Figure S5. Analysis of CRISPR/Cas9 mediated editing lines of *O3*.

(A) Gene structure of *O3* and sequencing of CRISPR/Cas9 target region in WT and T₀ plants. Scale bars, 0.5 kb.

(B) Appearance and transverse sections of mature seeds of wild type and *O3* knock out plants (*cr-1*~*cr-4*). Scale bars, 1mm.

(C) Relative expression level of *O3* in transgenic knock out plants (*cr-1*~*cr-4*).

(D) The grain length, grain width and grain thickness of brown rice of wild type and *O3* knock out plants (*cr-1*~*cr-4*).

Data in **(C-D)** are shown as mean \pm SD from three biological replicates. Asterisks indicate statistical significance as determined by Student's *t*-test (** $P < 0.01$).

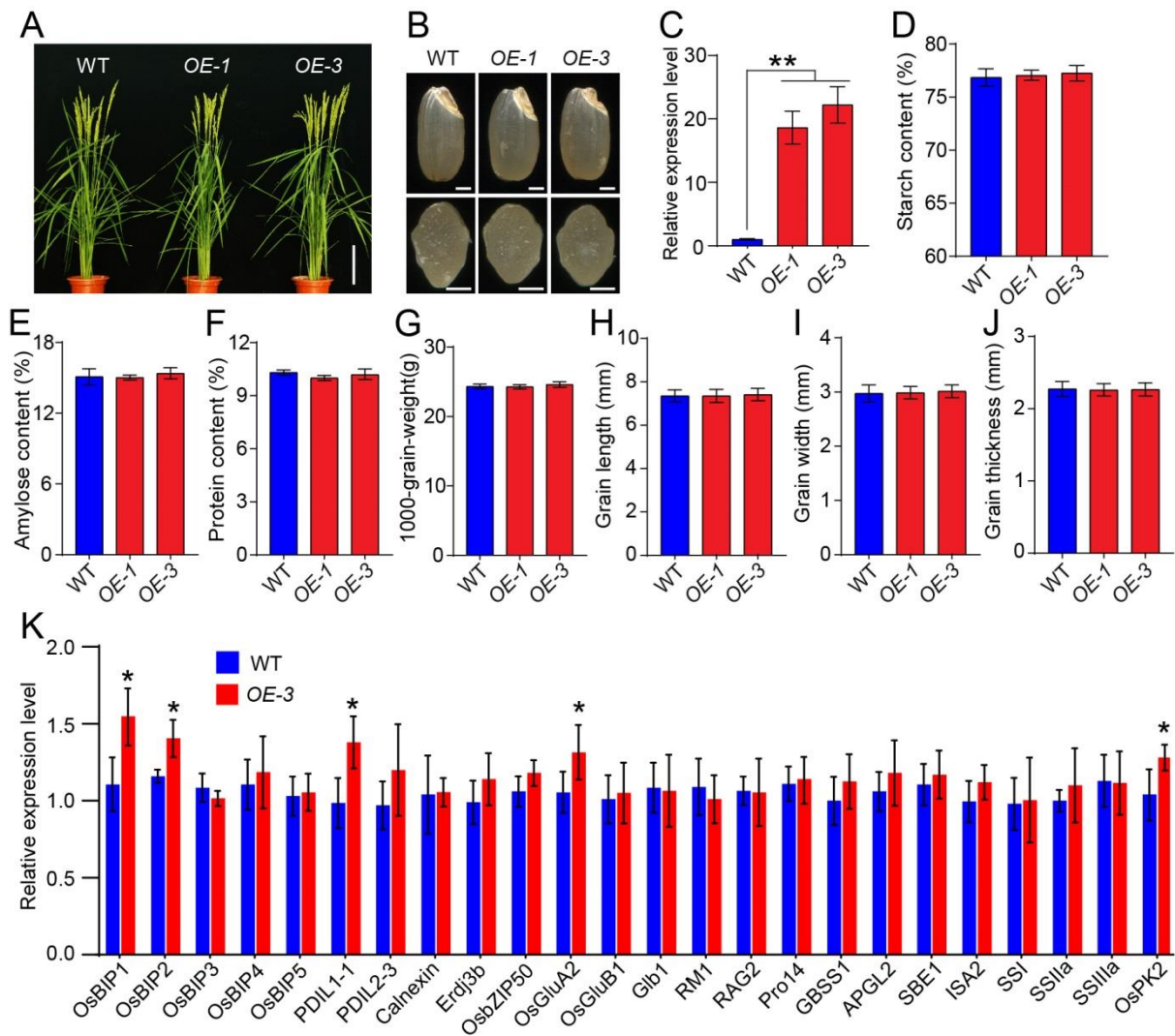


Figure S6. Analysis of overexpression lines of *O3* in WT background.

(A) The plant phenotype of WT and transgenic overexpression plants in WT background (*OE-1* and *OE-3*) after heading. Scale bar, 20 cm.

(B) Appearance and transverse sections of mature grains of WT, *OE-1* and *OE-3* plants. Scale bars, 1mm.

(C) Relative expression level of *O3* in *OE-1* and *OE-3*.

(D-G) The total starch (D), amylose (E), and total protein (F) content in endosperm, and 1000-grain-weight (G) of WT, *OE-1* and *OE-3*.

(H-J) The grain length (H), grain width (I) and grain thickness (J) of brown rice of WT, *OE-1* and *OE-3*.

(K) RT-qPCR analysis of genes related to ER stress, and genes related to starch and protein biosynthesis in WT and *O3 OE* lines.

Data in (C-K) are shown as mean \pm SD from three biological replicates, respectively. Asterisks indicate statistical significance as determined by a Student's *t*-test (* $P < 0.05$, ** $P < 0.01$).

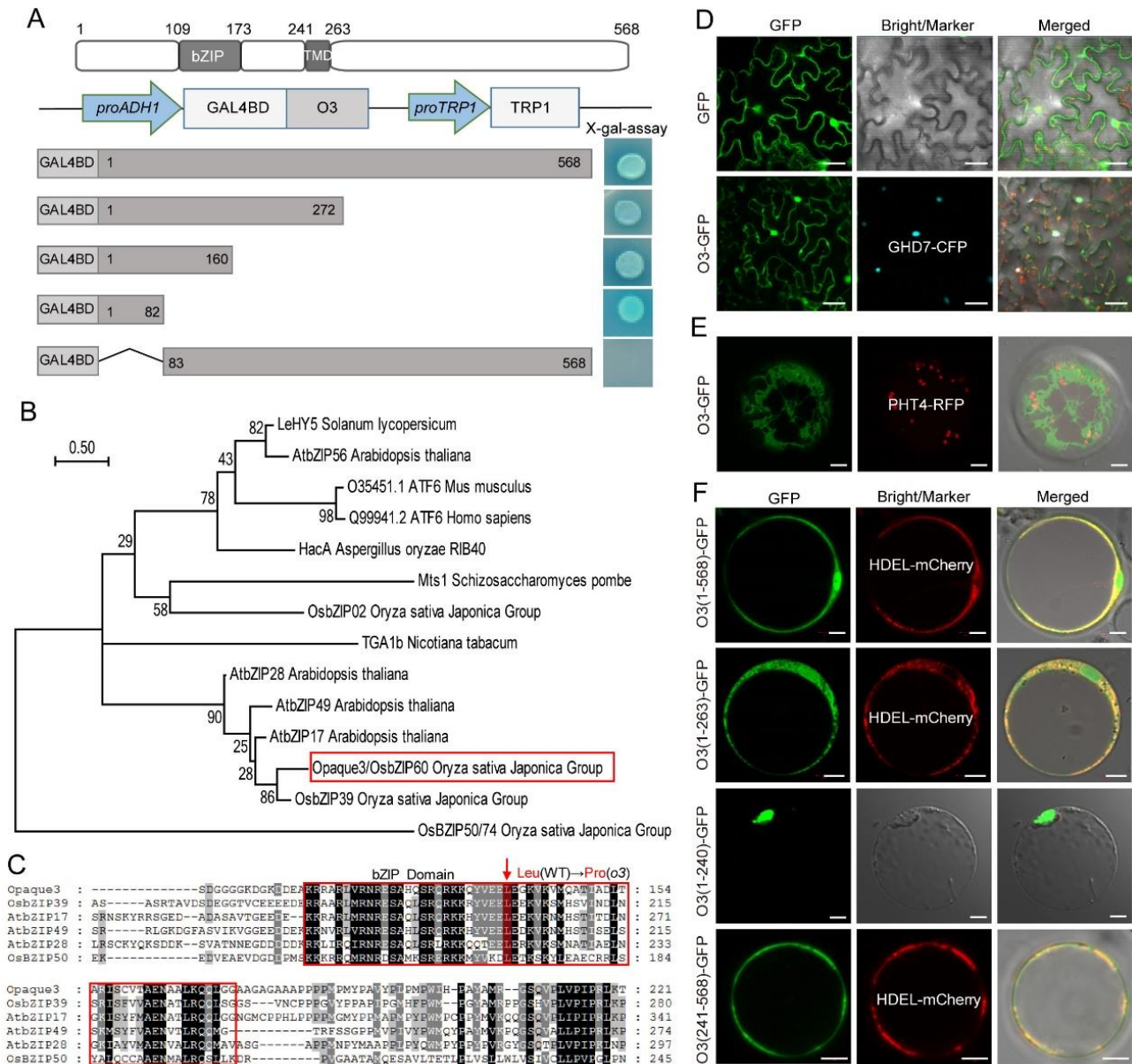


Figure S7. Molecular biological characteristics of O3

(A) Transactivation assay of different truncated form of O3. bZIP, TMD represented the basic zipper and transmembrane domain, respectively. Fusion proteins of the GAL4 DNA-binding domain and different portions of O3 were checked for their transactivation activity in yeast.

(B) Phylogenetic analysis of O3. The neighbor-joining tree was generated with MEGA7. Red box denotes the O3 in rice.

(C) Amino acid sequence alignment between part of O3 and other homologous proteins. It was generated with ClustalX2. White alphabet with black, grey background, and black alphabet with light grey background stands 100%, 80%, and 60% identity, respectively. Red box denotes the bZIP domain of O3 and other homologous proteins. Red arrow indicates the most conserved amino acid (lysine) of these homologous genes.

(D) Subcellular localization of O3-GFP in *N.benthamiana* leaves. O3-GFP is co-localized with GHD7-CFP in nucleus. Scale bars, 20 μ m.

(E) Subcellular localization of Full-length O3-GFP showing it is not co-localized with PHT4-RFP signal in Golgi. Scale bars, 5 μ m.

(F) Subcellular localization of different truncated forms of O3 in rice protoplast. O3^{1-240aa}-GFP is only localized in nucleus. O3^{1-263aa}-GFP and O3^{1-568aa}-GFP are co-localized in nucleus and ER. O3^{241-568aa}-GFP is only co-localized with HDEL-mCherry signal in ER. Scale bars, 5 μ m.

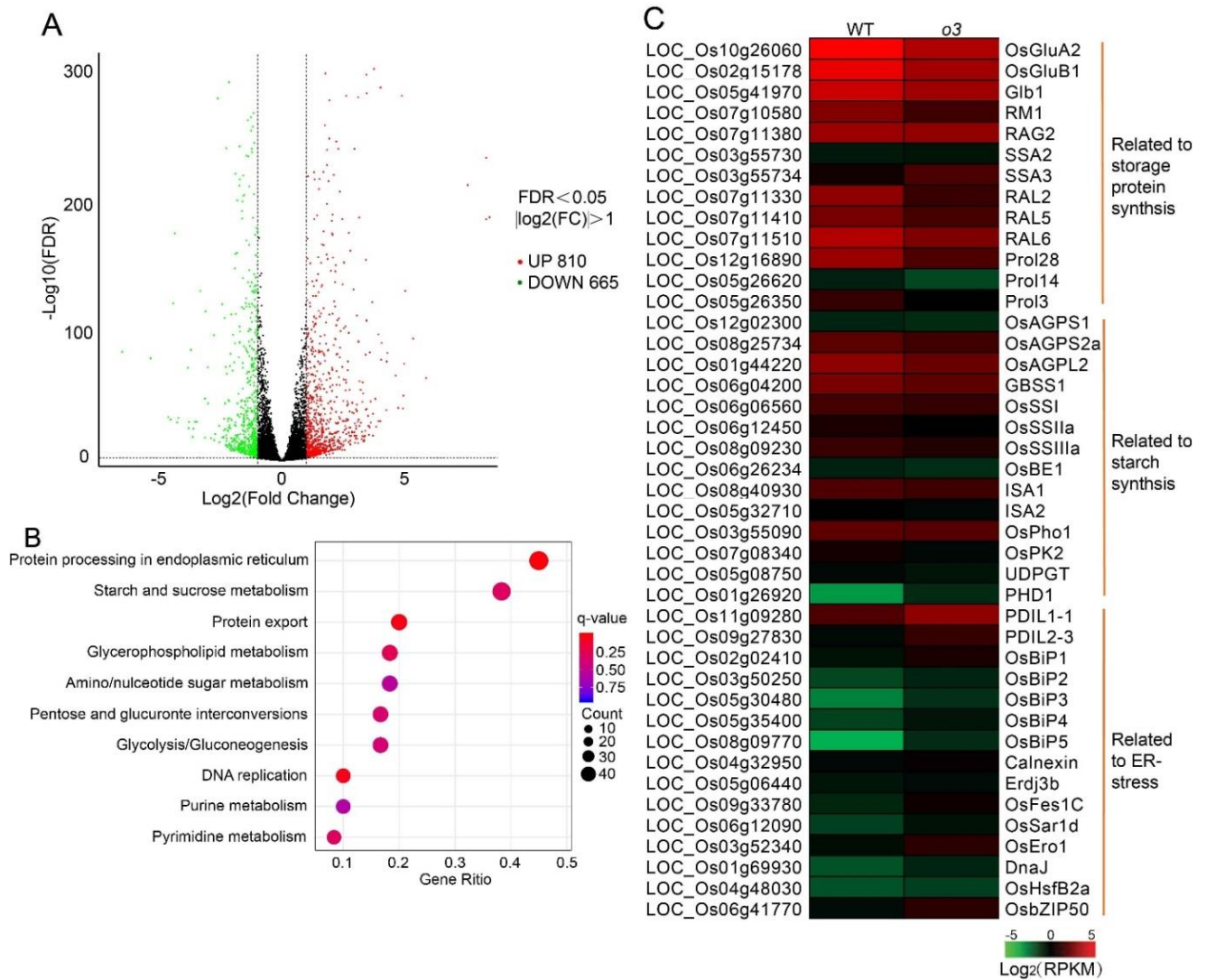


Figure S8. RNA-seq analysis of wild type and *o3* using grains at 12 DAF.

(A) Genes up- or down-regulated in RNA-seq data. A volcano plot of differential transcription levels between WT and *o3*. Green dots indicate reduced transcription level; red dots indicated increased transcription level; blue dots indicate no difference between WT and *o3*.

(B) GO enrichment terms for the 159 DEGs (differentially expressed genes) shared among the three groups.

(C) Heat map of the differentially regulated genes in WT and *o3* from RNA-seq. Genes related to ER stress were up-regulated while genes related to storage protein and starch synthesis were down-regulated. Data are shown as means \pm SD from three individual replicates.

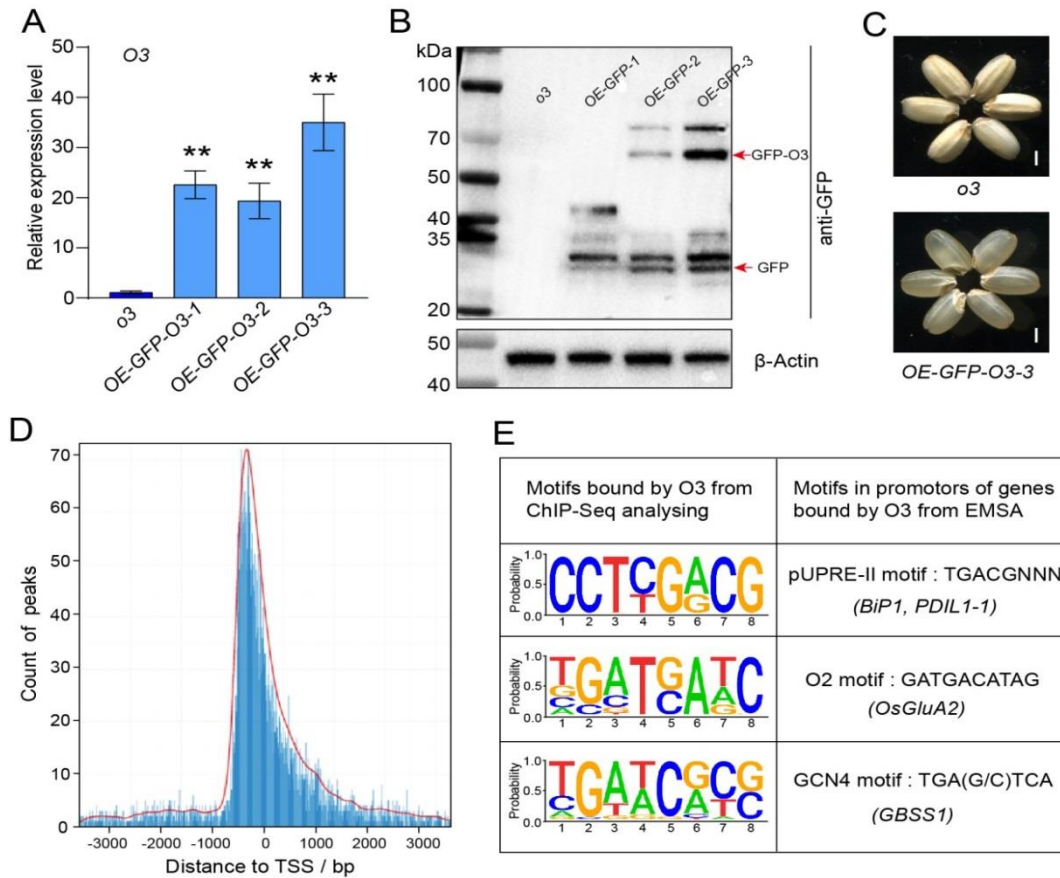


Figure S9. ChIP-seq analysis in grains at 9 DAF from *GFP-O3* overexpression lines.

(A) Relative expression level of *O3* in grains of *o3* mutant and *OE-GFP-O3* lines in *o3* background.

(B) The western blot detection of the GFP-O3 fusion protein level in 9-DAF grains of *o3* mutant and *OE-GFP-O3* overexpression lines using GFP antibodies.

(C) The appearance of mature grains of *o3* mutant and *OE-GFP-O3-3* line in *o3* background. *OE-GFP-O3-3* line was used for ChIP-seq. Scale bars, 1mm.

(D) Distribution of O3 binding peaks corresponding to the -3000bp to +3000bp region flanking the transcriptional start site (TSS).

(E) Three high-frequency motifs contained in the O3 binding peaks from ChIP-seq.

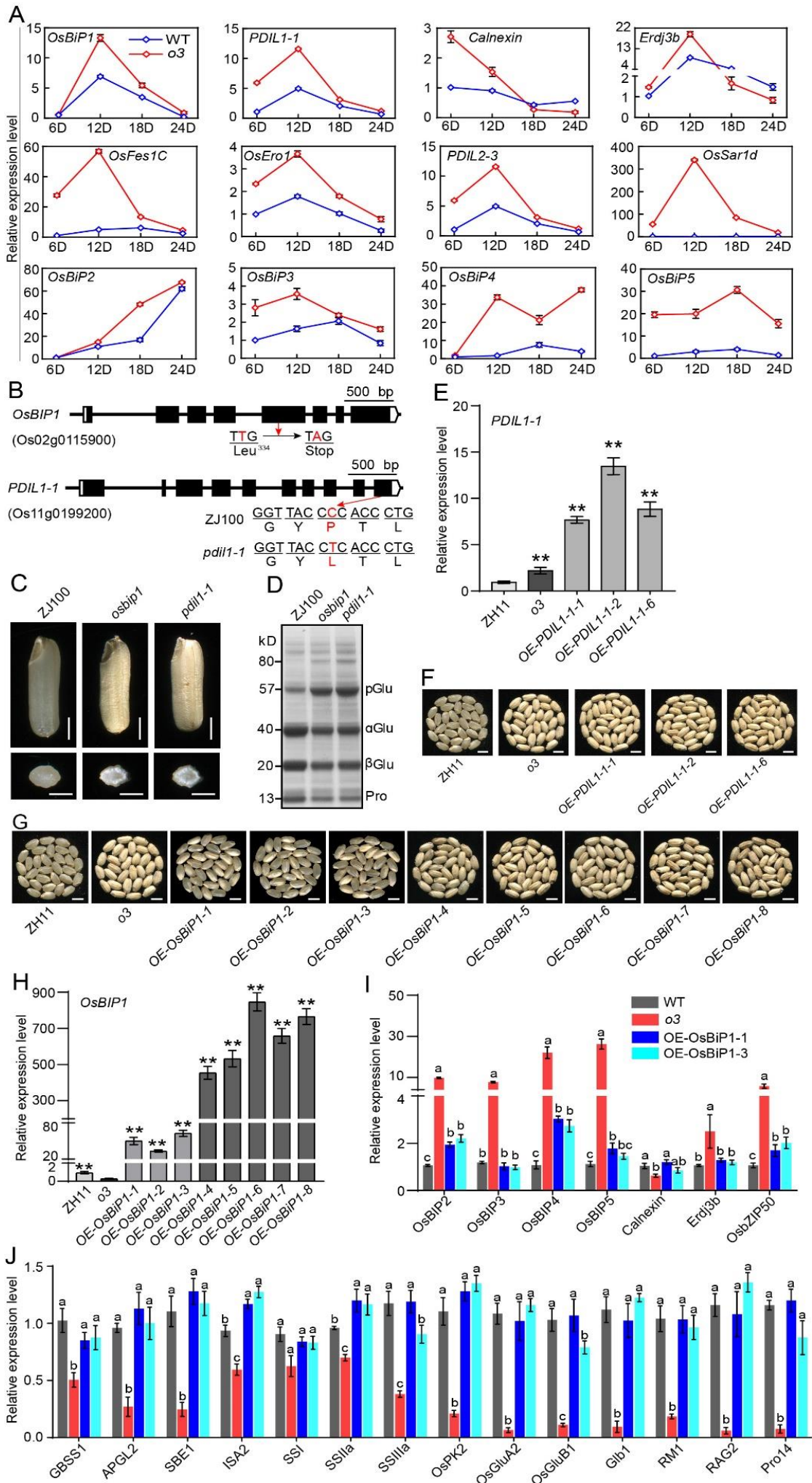


Figure S10. The grains phenotype of *osbip1* and *pdil1-1* mutant in ZJ100 background

(A) Relative expression level of genes (*OsBIP1*~*OsBIP5*, *PDIL1-1*, *PDIL2-3*, *Calnexin*, *Erdj3b*, *OsFes1C*, *OsEro1*, *OsSar1d*) related to ER stress in developing endosperm at 6, 12, 18, 24 days after fertilization.

(B) The mutation type of *OsBIP1* and *PDIL1-1* in ZhongJian100 (ZJ100) background.

(C) Grains appearance of *osbip1* and *pdil1-1* in ZJ100 background. Scale bars, 2mm.

(D) SDS-PAGE profiles of total dry-seed storage proteins of ZJ100, *osbip1*, and *pdil1-1* mutants. pGlu, 57-kDa proglutelins; α Glu, 40-kDa glutelin acidic subunits; β Glu, 20-kDa glutelin basic subunits; Pro, prolamins.

(E) RT-qPCR analysis of *PDIL1-1* transcription level in transgenic over-expression lines in the *o3* mutant background (*OE-PDIL1-1*).

(F) Grains appearance of *OE-PDIL1-1* lines. Scale bars, 5mm.

(G) Grains appearance of *OsBIP1* over-expression lines in the *o3* mutant background (*OE-OsBIP1*). *OE-OsBIP1-1*~*3* could partly restore the transparent endosperm phenotype, but *OE-OsBIP1-4*~*8* failed to rescue the *o3* phenotype. Scale bars, 5mm.

(H-J) RT-qPCR analysis of *OsBIP1* (**H**), genes related to ER stress (**I**), and genes related to starch and protein biosynthesis (**J**) in *OE-PDIL1-1* lines.

Data in **(A, E, H-J)** are shown as means \pm SD from three individual replicates. Statistically significant differences were determined using Student's *t*-test (indicated with different lowercase letters ($P < 0.05$), or * $P < 0.05$; **, $P < 0.01$).

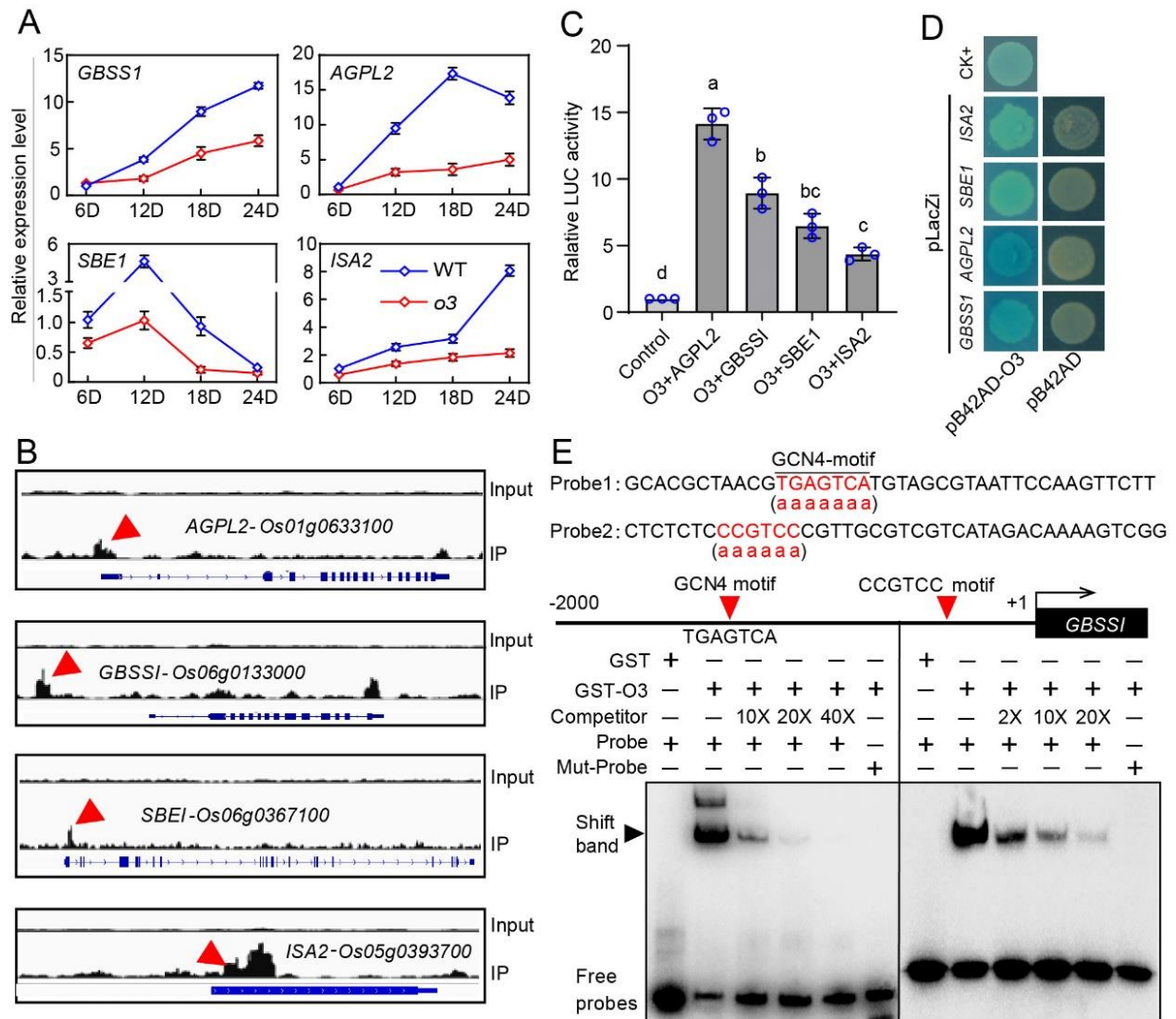


Figure S11. O3 directly activate the transcription of genes related to starch synthesis.

(A) RT-qPCR analysis of *GBSS1*, *AGPL2*, *SBE1*, and *ISA2* transcription level in developing endosperm at 6, 12, 18, 24 days after fertilization. Data are shown as means \pm SD (n=3).

(B) Chip-seq results showing the distributions of O3 binding sites for *GBSS1*, *AGPL2*, *SBE1*, and *ISA2* loci, as shown in Integrative Genomics Viewer. Red arrowhead indicates significant peaks calculated by MACS2, and the positions of peaks were shown in Attachment data II. Input sample was used as a negative control.

(C) Luciferase transient transactivation assay in rice protoplasts. O3 significantly activated the transcription of *GBSS1*, *AGPL2*, *SBE1* and *ISA2*. Data are shown as means \pm SD (n=3), significant difference was labeled with different letters according to Student's *t*-test.

(D) Yeast-one-hybrid assay showing the binding of O3 to the promotor of *GBSS1*, *AGPL2*, *SBE1*, *ISA2*.

(E) EMSA showed that O3 could bind to the probes of *GBSS1* with GCN4-motif (probe1, left) and CCGTCC-motif (probe2, right), the mutated motif in mut-probes was showed in bracket.

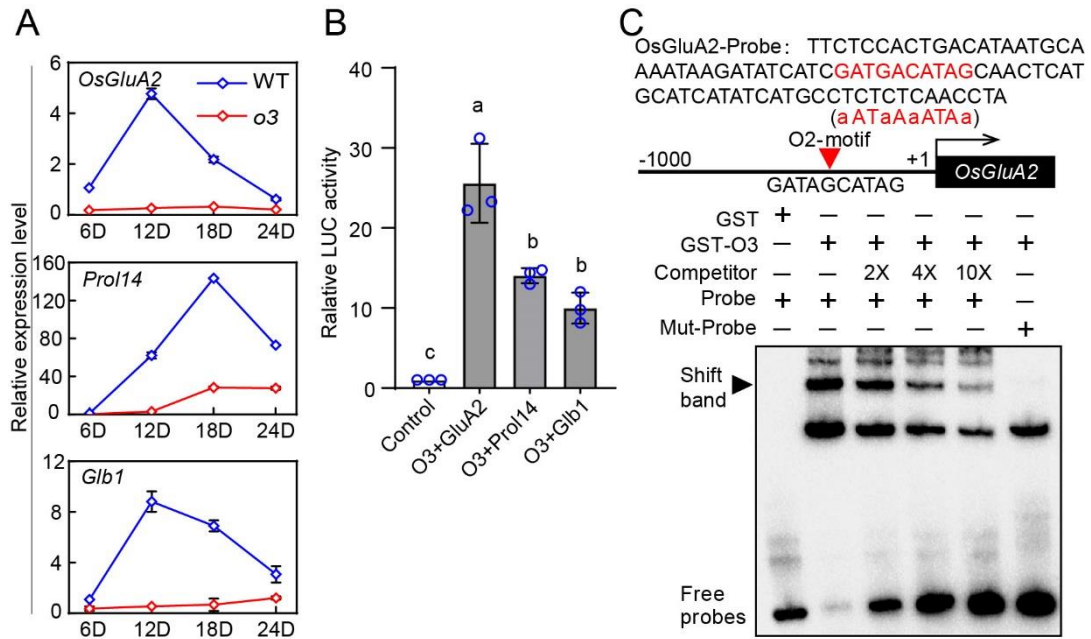


Figure S12. O3 directly activate the expression of genes related to protein synthesis.

(A) RT-qPCR analysis of *OsGluA2*, *Prol14*, and *Glb1* transcription level in developing endosperm at 6, 12, 18, 24 from 6~24 days after fertilization. Data are shown as means \pm SD (n=3).

(B) Luciferase transient transactivation assay in rice protoplasts. O3 significantly activated the transcription of *OsGluA2*, *Prol14*, and *Glb1*. Data are shown as means \pm SD (n=3), significant difference was labeled with different letters according to Student's *t*-test (n=3).

(C) EMSA showed that O3 could bind to the probes of *GBSS1* with O2-motif; the mutated motif in mut-probes was showed in bracket.

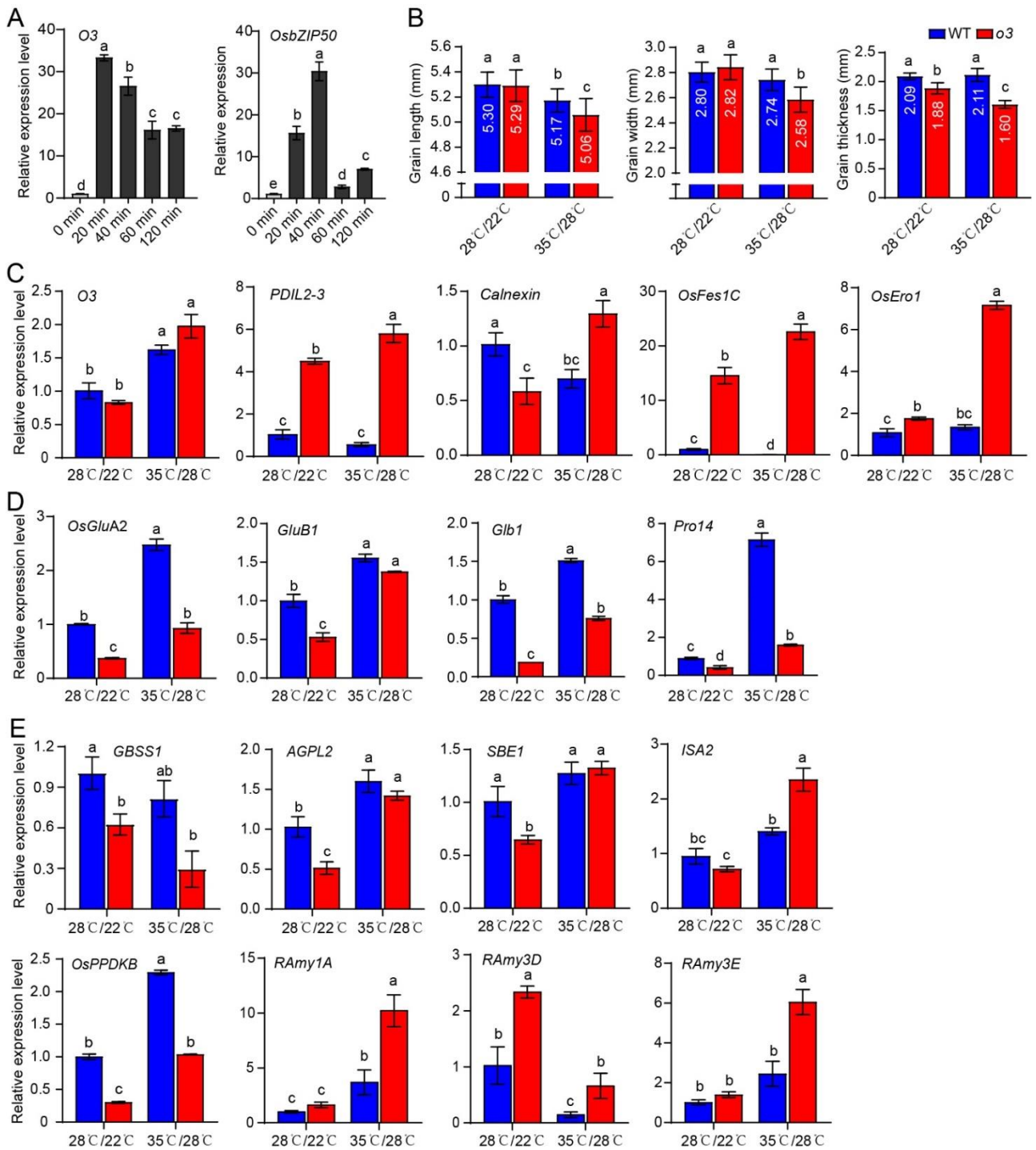


Figure S13. *o3* undergo more serious ER stress under high-temperature conditions.

(A) Relative expression level of *O3* and *OsbZIP50* in 2-week-old seedlings under heat stress treatment (42°C).

(B) Grain length, grain width and grain thickness of WT and *o3* under high-temperature treatment (35°C, 12h light /28°C, 12h, Dark) and normal-temperature treatment (28°C, 12h light /22°C, 12h, Dark).

(C-E) Relative expression levels of genes related to ER stress **(C)**, protein synthesis **(D)** and starch synthesis **(E)**.

Values are means \pm SD from three biological replicates. Significant difference was labeled with different letters according to Student's *t*-test.

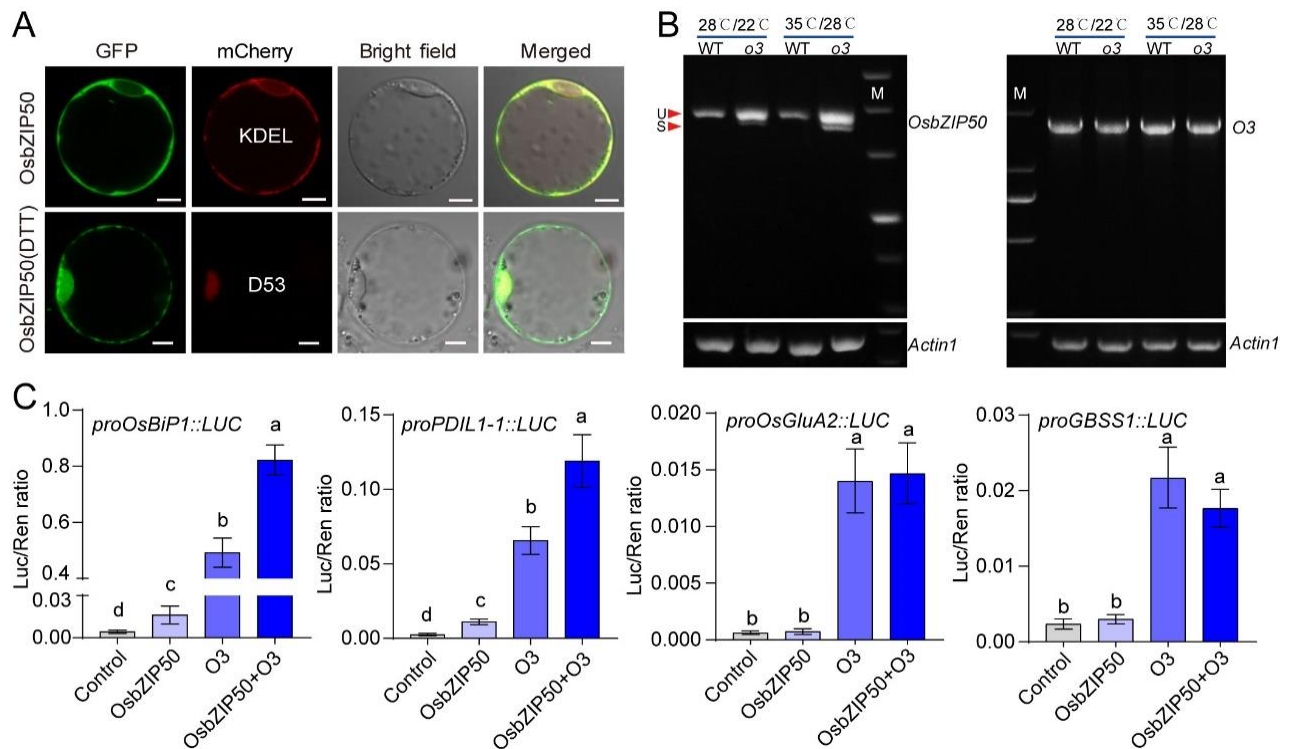


Figure S14. OsbZIP50 can assist O3 in response to the ER stress.

(A) Subcellular localization of OsbZIP50 in rice protoplast. OsbZIP50-GFP was localized in cytoplasm and co-localized with HDEL-mChery signal in ER. OsbZIP50-GFP was co-localized with DWARF53(D53)-mChery signal in nucleus after 2 hours Dithiothreitol (DTT) treatment. Scale bars, 5 μ m.

(B) The splicing forms of *OsbZIP50* and *O3* mRNA were detected in the wild type and *o3* mutant. The semi-quantitative RT-PCR analysis of *OsbZIP50* and *O3* transcripts in endosperm cells of WT and *o3* under high- and normal-temperature conditions. U, un-spliced form; S, spliced form.

(C) Transactivation assay of OsbZIP50 and O3 for *OsBIP1*, *PDIL1-1*, *OsGluA2*, and *GBSS1* in rice protoplasts. Luciferase reporter assay shows that OsbZIP50 can enhance the transient transactivation of *OsBIP1* and *PDIL1-1* together with O3. Values are means \pm SD from three biological replicates. Significant difference was labeled with different letters according to Student's *t*-test.

Table S1. Primers used in this study

Mapping	RM22097-F	AAGAAATTCAAACACATGA
	RM22097-R	AAAACATCTACTTTGATCCA
	RM22166-F	TCCTTGTAATCTGGTCCC
	RM22166-R	GTAGCCTAGCATGGTGCATG
Sequencing	03-F	CGCACCTTCGCTCTCTTTCC
	03-R	ACCTGCGAGCCACGCATTGC
	OsbZIP39-F	ATGGCGGAGCCGGCCCTGCTG
	OsbZIP39-R	GCACTTGGCCGCTCCGAGCT
	OsbZIP50-F	GGCAACCCACCGGAGAGAC
	OsbZIP50-R	CTCTCCCTCGATTTTCATGGC
Binary vector construction	1300-O3-KpnI-F	AATTCGAGCTCGGTACCAGGCGCAATTGCCTTATGAAG
	1300-O3-SalI-R	GCATGCCTGCAGGTCGACTTGGAAACGCGAAAACCTCAG
	RHV-O3-SacI-F	GGATCCCCGGGTGAGCTCATGGCGGAGCCGGACCTACTC
	RHV-O3-HindIII-R	GCCGCACTAGTAAGCTTCAAGTGAGGGCTATGGCTTTTG
	GUS-O3-EcoRI-F	CCATGATTACGAATTCAGGAGTCCTGGTCATCTTCT
	GUS-O3-NcoI-R	CTCAGATCTACCATGGCCAGATCGTCGAGATCGAAA
Crispr Cas9	Crispr-O3-Target1-F	ggcACCCCGACTTCCCGACCCTCG
	Crispr-O3-Target1-R	aaacCGAGGGTCGGGAAGTCGGGG
	Crispr-O3-Target2-F	ggcAGGGAGAGCGCGCACCAGTCCG
	Crispr-O3-Target2-R	aaacCGACTGGTGCAGCTCTCCC
	Crispr-OsbZIP39-F	ggcGGGCTCGAGTTCGACCTGCC
	Crispr-OsbZIP39-R	aaacGGCAGGTCGAACTCGAGCC
	Crispr-OsbZIP50-F	gttGAGTGAGGCGGGGGAAGCA
	Crispr-OsbZIP50-R	aaacTGCTTCCCCCGCTCACT
Subcellular localization	PAN580-O3-XbaI-F	AGTCCGGAGCTAGCTCTAGAATGGCGGAGCCGGACCTACT
	PAN580-O3-BamHI-R	CCCTTGCTACCATGGATCCCAAGTGAGGGCTATGGCTTT
	PAN580-O3(1-240)-BamHI-R	CCCTTGCTACCATGGATCCCTTCTTGGTCTTCCGGGCCTT
	PAN580-O3(1-263)-BamHI-R	GTCCGGAGCTAGCTCTAGAAATCGGATGTATGGTGCAGCG
	PAN580-OsbZIP50-XbaI-F	AGTCCGGAGCTAGCTCTAGAATGACATGGCACATTC AAGC
	PAN580-OsbZIP50-BamHI-R	CCCTTGCTACCATGGATCCGCAAGCAGCTGCTGCTAAAC
	pYBA1132-O3-XbaI-F	GGTGGCGCCGCTCTAGAATGGCGGAGCCGGACCTACT
	pYBA1132-O3-KpnI-R	CTTGCTACCATGGTACCAAGTGAGGGCTATGGCTTT
	mCherry-D53-F	AGCCCAGATCACTAGTATGCCCACTCCGGTGGCCGCC
	mCherry-D53-R	TGCTCACCATGGATCCACAATCTAGAATTATCTTTGGC
Protein expression	GST-O3-domain-F	CGTGGATCCCCGGAATTCGGCAAGGATGGGAAGGATGAT
	GST-O3-domain-R	CGATGCGGCCGCTCGAGACCGGCGGCCACCCAATTG
Chip-qPCR	Chip-OsBIP1-F1	GGCCTGTTGAGATTGTTGCA
	Chip-OsBIP1-R1	AAGGGTTGTTTCAGATTACTGT
	Chip-OsBIP1-F2	ATTTGTGATGGCAAATCCACG
	Chip-OsBIP1-R2	CTGGTCGGGACCCGTTTACT
	Chip-OsBIP1-F3	ACGCCCAGTAAACGGGTCC
	Chip-OsBIP1-R3	TATAAGGGGAGATGACTTGA
	Chip-OsBIP1-F4	TCGCCACGAACCCATAAA
	Chip-OsBIP1-R4	CCACCACCACACGCGCT
	Chip-PDIL1-1-F1	CGATCGGGACCACCCGGTG
	Chip-PDIL1-1-R1	GGATACGATAAAAGCTGTGT
	Chip-PDIL1-1-F2	CTAATTTACCCGGATCCGGA

	Chip-PDIL1-1-R2	CGACTACGTACACGTACCTG
	Chip-PDIL1-1-F3	TGACGTGGCGTTGGCCGTCG
	Chip-PDIL1-1-R3	ATGCCCCTGATGAGGAGTGA
	Chip-PDIL1-1-F4	CCTCTAGTTTTAGCACATCTC
	Chip-PDIL1-1-R4	CTGAGACGACACGCTTCTCA
LUC assay	None-O3-EcoR1-F	TAGAACTAGTGGATCCATGGCGGAGCCGGACCTACT
	None-O3-BamH1-R	GCTTGATATCGAATTCTTACAAGTGAGGGCTATGGCT
	190LUC-AGPL2-F	GGCCAGTGCCAAGCTTCGTATGCCCTAGGTGCACCAAC
	190LUC-AGPL2-R	AGGGTCTTGCAGATCTTTGTGCACAAGCATTCTGATCC
	190LUC-SBE1-F	GGCCAGTGCCAAGCTTACATATGCCTTTGTGCCGGGA
	190LUC-SBE1-R	AGGGTCTTGCAGATCTGGAGGAGGAAGAGGAGGTGAG
	190LUC-ISA2-F	GGCCAGTGCCAAGCTTTAGATGGCCTCTAGGGTGTG
	190LUC-ISA2-R	AGGGTCTTGCAGATCTCTTTTCGCACGGCTATTTTCG
	190LUC-GBSS1-F	GGCCAGTGCCAAGCTTCCGCTGGCACCCGGAGGACTA
	190LUC-GBSS1-R	AGGGTCTTGCAGATCTGTACGTCGCTCGCGTGTGCT
	190LUC-OsBiP1-F	GGCCAGTGCCAAGCTTGGGCCTGTTGAGATTGTTGCAATT
	190LUC-OsBiP1-R	AGGGTCTTGCAGATCTACGCGCATCCGCGAACCCGAT
	190LUC-PDIL1-1-F	GGCCAGTGCCAAGCTT CGGATCTGCCATCTGTGACT
	190LUC-PDIL1-1-R	AGGGTCTTGCAGATCTGAGACGACACGCTTCTCACA
	190LUC-GluA2-F	GGCCAGTGCCAAGCTTTGCTACAACCTACCAGTCCA
	190LUC-GluA2-R	AGGGTCTTGCAGATCTCCATCGACAAGAGGAACAA
	190LUC-Glb1-F	GGCCAGTGCCAAGCTTTAGCCATTGCACATGGAGTT
	190LUC-Glb1-R	AGGGTCTTGCAGATCTCGACCTTGTAGCCATTGAT
	190LUC-Pro114-F	GGCCAGTGCCAAGCTTCAAAGAATAGGTCAATTCCACCCA
190LUC-Pro114-R	AGGGTCTTGCAGATCTATAGCAAGGAGAGCAAAGACGAA	
Yeast one-hybrid assays	pB42AD-O3-EcoRI-F	TGCCTCTCCGAATTCATGGAGCACGTGTTCCCGTC
	pB42AD-O3-EcoRI-R	CGAGTCGGCCGAATTCCTACTGAAGCTCCATGTTGAC
	pLacZi-GBSS1-XhoI-F	ATCTGTGCACCTCGAGCCCTTTGTGCAGGCGTTAGT
	pLacZi-GBSS1-XhoI-R	GAGCACATGCCTCGAGACACATTTTACCCGGTCCCC
	pLacZi-AGPL2-F	GAGCACATGCCTCGAGTCTATAGAGGGGAAGGCTGCA
	pLacZi-AGPL2-R	GAGCACATGCCTCGAGAAGCTGGTGGACAGGTAGATC
	pLacZi-SBE1-F	GAGCACATGCCTCGAGACATATGCCTTTGTGCCGGGA
	pLacZi-SBE1-R	GAGCACATGCCTCGAG AGGCTCATTAGATTCTGCTCTCGCA
	pLacZi-ISA2-F	GAGCACATGCCTCGAGTAGATGGCCTCTAGGGTGTG
	pLacZi-ISA2-R	GAGCACATGCCTCGAG CTTTTTCGCACGGCTATTTTCG
EMSA	EMSA-OsBIP1-F	TGGTCCAGGTCAGACTCATGACGTCCC GGCCAACGCGACG
	EMSA-OsBIP1-R	CGTCGCGTTGGCCGGGACGTCATGAGTCTGACCTGGACCA
	EMSA-PDIL1-F	AGCCTCGTGGAGGGATGATTTGACGATGATAAGTACAGGG
	EMSA-PDIL1-R	CCCTGTACTTATCATCGTCAAATCATCCCTCCACGAGGCT
	EMSA-GBSS1-F	GCACGCTAACGTGAGTCATGTAGCGTAATTCCAAGTTCTT
	EMSA-GBSS1-R	AAGAACTTGAATTACGCTACATGACTCACGTTAGCGTGC
	EMSA-GBSS1-F1	CTCTCTCCCGTCCC GTTGCGTGTCATAGACAAAAGTCCGG
	EMSA-GBSS1-R1	CCGACTTTTGTCTATGACGACGCAACGGGACGGGAGAGAG
	EMSA-OsGluA2-F	TTCTCCACTGACATAATGCAAAAATAAGATATCATCGATGACATAG CAACTCATGCATCATATCATGCCTCTCTCAACCTA
	EMSA-OsGluA2-R	TAGGTTGAGAGAGGCATGATATGATGCATGAGTTGCTATGTCATC GATGATATCTTATTTTGCATTATGTCAGTGGAGAA
qRT-PCR	Ubiquitin-F	TGGTCAGTAATCAGCCAGTTTGG

Ubiquitin-R	GCACCACAAATACTTGACGAACAG
q-SSI-F	GGGCCTTCATGGATCAACC
q-SSI-R	CCGCTTCAAGCATCCTCATC
q-SSIIa-F	GCTTCCGGTTTGTGTGTCA
q-SSIIa-R	CTTAATACTCCCTCAACTCCACCAT
q-SSIIIa-F	GCCTGCCCTGGACTACATTG
q-SSIIIa-R	GCAAACATATGTACACGGTTCTGG
q-SSIVa-F	GGGAGCGGCTCAAACATAAA
q-SSIVa-R	CCGTGCACTGACTGCAAAAT
q-GBSSI-F	AACGTGGCTGCTCCTTGAA
q-GBSSI-R	TTGGCAATAAGCCACACACA
q-AGPL1-F	GGAAGACGGATGATCGAGAAAG
q-AGPL1-R	CACATGAGATGCACCAACGA
q-AGPL2-F	AGTTCGATTCAAGACGGATAGC
q-AGPL2-R	CGACTTCCACAGGCAGCTTATT
q-AGPS1-F	GTGCCACTTAAAGCACCATT
q-AGPS1-R	CCCACATTCAGACACGGTTT
q-AGPS2b-F	AACAATCGAAGCGCGAGAAA
q-AGPS2b-R	GCCTGTAGTTGGCACCCAGA
q-SBEI-F	TGGCCATGGAAGAGTTGGC
q-SBEI-R	CAGAAGCAACTGCTCCACC
q-ISA2-F	ATGCCAATGCCGTTTCTCTC
q-ISA2-R	GTGGATGTACGGATCGAGGT
q-PUL-F	ACCTTTCTTCCATGCTGG
q-PUL-R	CAAAGGTCTGAAAGATGGG
q-PHOL-F	TTGGCAGGAAGTTTCGCT
q-PHOL-R	CGAAGCCTGAAGTGAACCTTGCT
q-GluA2-F	ACAAGAGAAGGATGTGCTTAC
q-GluA2-R	ATTCTTTATCCGCATTGCCAAC
q-GluB1-F	CAAGACAAACGCTAACGCCTTC
q-GluB1-R	TCGATAATCCTGGGTAGTATTG
q-GluD-F	AAAGACAATTTCCGACCCTACG
q-GluD-R	TTAGGAAGTGGTAACCCCGCTG
q-Glb1-F	AGGTTCCAGCCGATGTTCC
q-Glb1-R	CATGCTCTCCTCGTAGCTCCTC
q-RM1-F	TTGTGCAGCAACTACAGCTG
q-RM1-R	CGGAGCAATGTAGTAGTTAG
q-Pro14-F	ACAACCTCCAGCAGTTTGGTG
q-Pro14-R	CAAGGGTGGTAATGGTACTG
q-RP10-F	CAGTTGCCAGATGATGCAGAG
q-RP10-R	TCAACAACAACCACAGGAAGAGA
q-RAG1-F	GTTCTCGGTATTGCTCCTCGT
q-RAG1-R	GGCTGTAGACTTGGTGGTGGT
q-OsBiP1-F	TGGAAAGCTGAGGAGGGAAG
q-OsBiP1-R	CTTGACAGGTCCCATGGTCT
q-OsBiP2-F	ATCTCCCGTACAAGGTGGTG
q-OsBiP2-R	CTCGGCTGTCTCCTTCATCT
q-OsBiP3-F	TACGTCTACGGCGTCAAGAA

	q-OsBiP3-R	GGAGCTTCTCCTCGTACTCC
	q-OsBiP4-F	ATGGACCACTTCGTCAAGGT
	q-OsBiP4-R	GTCGAACAGGGACTCGATCT
	q-OsBiP5-F	AGAGCATGATCCTCCTCGAC
	q-OsBiP5-R	CGTCTGCTGTGCCTTGTACG
	q-Calnexin-F	AGGAGCTTGATGAGCCTGTT
	q-Calnexin-R	CTCAAGGCCATTCTGAAGCC
	q-PDIL1-1-F	GTGCTGCTGAGGAGTTCAAG
	q-PDIL1-1-R	CCTCAGCCCAAAGTACTGGA
	q-PDIL2-3-F	GCAAGTTGGAGTTGGTGGTT
	q-PDIL2-3-R	GGGTACCGTCCAAAGGAAGA
	q-ERdj3B-F	TCATAAAGCCAGCACCAGGA
	q-ERdj3B-R	CAGACCTGCTCGGTCATTTG
	q-SDF2-F	GGTTGCGCCATGTTGATACT
	q-SDF2-R	TACCTCTTGCTGTCCACCAG
	q-Ero1-F	TGTGTCGGCTTAGGGATTGT
	q-Ero1-R	GGCTTCTTGAATGGCTCAGG
	q-Fes1C-F	AAAGAACAGGCAGAGGGTGT
	q-Fes1C-R	TGCCGATCCTCCAGTCAAAT
	q-Sar1d-F	GAGCAGGAGCTGTGCTACTA
	q-Sar1d-R	TGACATCCACCTGAAGCCAT
	q-OsbZIP50-F	GGAAGGAGAATGAGGTGGCT
	q-OsbZIP50-R	TCCCTCGATTTCATGGCAGA
	q-OsbZIP39-F	TCCAAGGGAGGCTGGTAATG
	q-OsbZIP39-R	GGAGCTCTTGAAAGGAAGCG
semi-RT	RT-Actin1-F	CCAAGGCCAATCGTGAGAAG
	RT-Actin1-R	AAGGAAGGCTGGAAGAGGAC
	OsbZIP50-S-F	GAGCAAGAAGAAGAGGAGGC
	OsbZIP50-S-F	CTTCTTTCCGGTTACCGTCG